Progress In Electromagnetics Research B, Vol. 4, 147–158, 2008

ANALYSIS OF A GAP-COUPLED STACKED ANNULAR RING MICROSTRIP ANTENNA

J. A. Ansari, R. B. Ram, and P. Singh

Department of Electronics and Communication
University of Allahabad
Allahabad 211002, India

Abstract—A theoretical analysis of a gap-coupled stacked annular ring microstrip antenna with superstrate is performed in order to obtain wider bandwidth operation. The effects of air gap, superstrate thickness and feeding point location on the antenna performance are analyzed in TM_{11} mode using equivalent circuit concept. It is noted that the proposed antenna is very sensitive to the feeding point location in TM_{11} mode while annular ring microstrip patch antenna is independent of feed point in that mode. The optimized proposed antenna shows an impedance bandwidth of 13.96% whereas the antenna without air-gap has 8.75% bandwidth and without superstrate it has bandwidth of 10.89%. The theoretical results are compared with simulated and experimental results.

1. INTRODUCTION

Microstrip patch antennas are becoming popular because of their numerous advantages such as their low profile, conformability, low fabrication cost, mechanical robustness, polarization agility, compatibility/easy integration with microstrip circuits/solid state devices and adaptability to active antenna elements. Although, in principle, the patch may be of any shape yet, in practice, only simple geometries like rectangular, square and circular structures are commonly employed. Like rectangular and circular patches, the annular ring microstrip antenna (ARMSA) has received the considerable attention of several investigators [1–8] due to its many salient features such as small size and broader bandwidth compared to other conventional patches. However, the main obstacle that restricts its wide applications in various fields is its inherent narrow bandwidth and low gain [1].

Therefore, a number of bandwidth extension techniques have been suggested to achieve better performance of the ARMSA including use of thick substrate [2], use of air gap [3], use of superstrate [4], use of parasitic elements [5–7] and integration of active devices [8]. Among these techniques, the stacked parasitic configuration has been selected because it provides close spacing between the elements that is not realized in single layer parasitic elements, it does not excite surface waves that occur in thick dielectric substrate, and it does not generate high order modes that are generated for low dielectric substrate [7]. In this paper, the theoretical investigation of a gap-coupled stacked annular ring microstrip antenna is presented in which foam material introduces an air gap between the fed and parasitic patches. The results obtained are compared with simulated (IE3D) and experimental [5] results.

2. ANTENNA DESIGN AND THEORETICAL CONSIDERATIONS

The geometrical configuration of the proposed antenna is shown in Fig. 1. It consists of a probe fed annular ring and a parasitic circular disc. The inner and outer radii of the ring are $a = 8.81\,\text{mm}$ and $b = 21.2\,\text{mm}$, respectively. The radius of the disc ($R_d = 24.39\,\text{mm}$) is taken slightly greater than the outer radius of the ring to impose a different but close resonance frequency to the resonance frequency of the ring. The fed and parasitic patches are etched on a dielectric substrate of relative dielectric constant $\varepsilon_{r1} = \varepsilon_{r3} = 2.2$ and thickness $h_1 = h_3 = 1.59\,\text{mm}$. A foam substrate of relative permittivity $\varepsilon_{r2} = 1.06$ and thickness $h_2 = 3.18\,\text{mm}$ has been introduced between the two patches to provide air gap-coupling between them when the fed patch is excited by a 50 ohm coaxial probe of radius 1.25 mm. The probe is located very close to the inner radius of the ring such that its distance from the center of the ring is $Y_0 = 9.45\,\text{mm}$. Moreover,

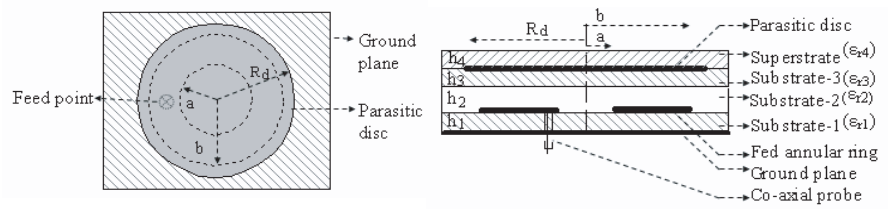

(a) Top view (b) Side view

Figure 1. Geometry of the proposed antenna.

a superstrate of relative dielectric constant $\varepsilon_{r4} = 2.2$ and thickness $h_4 = 3.18\,\text{mm}$ covers the parasitic patch to protect the antenna from environmental hazards. The bottom patch is so designed that it can operate at 2.30 GHz.

Due to the presence of the parasitic patch, the proposed stacked structure behaves as an antenna having two resonance frequencies. One resonance frequency is associated with the resonator formed by the fed annular ring and second one is associated with the resonator formed by the parasitic disc. Due to the presence of superstrate the effective dielectric constant for the two resonators are changed causing change in their resonance behaviors. The dielectric substrate in three layers above the annular ring can be considered as a superstrate of relative dielectric constant ε_{rs} that can be given as [9]

$$\varepsilon_{rs} = \frac{\sum_{i=2}^{4} h_i}{\sum_{i=2}^{4} \frac{h_i}{e_{ri}}} \tag{1}$$

Therefore, the effective dielectric constant for the first resonator is given as [10]

$$\varepsilon_{ef} = \varepsilon_{r1} q_1 + \varepsilon_{rs} \frac{(1-q_1)^2}{\varepsilon_{rs}(1-q_1-q_2)+q_2} \tag{2}$$

where q_1 and q_2 are the filling factors defined as [10].

The effective dielectric constant with superstrate can be represented as a single patch with semi-infinite superstrate with relative dielectric constant equal to unity and a single relative dielectric constant equal to ε_{rf} which is given as [10]

$$\varepsilon_{rf} = \frac{2\varepsilon_{ef} - 1 + A_f}{1 + A_f} \tag{3}$$

where $A_f = \left(1 + \frac{12h_1}{w}\right)^{-1/2}$; $w = b - a$.

Therefore, the resonance frequency of the first resonator is given as

$$f_{fnm} = \frac{X_{nm} c}{2\pi a \sqrt{\varepsilon_{ef}}} \tag{4}$$

where X_{nm} is the mth zero of $J_n'(2X_{nm})\,Y_n'(X_{nm}) - J_n'(X_{nm})\,Y_n'(2X_{nm})$ and c is the velocity of light in free space.

In the similar fashion, the equivalent relative dielectric constant of the all three layers of the substrate below the parasitic disc can be given as

$$\varepsilon_{rd} = \frac{\sum_{i=1}^{3} h_i}{\sum_{i=1}^{3} \frac{h_i}{e_{ri}}} \tag{5}$$

The effective dielectric constant for the second resonator with the superstrate can be given as

$$\varepsilon_{ed} = \varepsilon_{rd} q_1' + \varepsilon_{r4} \frac{(1 - q_1')^2}{\varepsilon_{r4}(1 - q_1' - q_2') + q_2'} \tag{6}$$

where q_1' and q_2' are the filling factors for the parasitic patch.

Therefore, the resonance frequency of the second resonator is given as

$$f_{dnm} = \frac{x_{nm}\, c}{2\pi R_{de}\sqrt{\varepsilon_{ed}}} \tag{7}$$

where x_{nm} is the mth zero of $J_n'(kR_d)$ and $x_{nm} = kR_d$; k is the wave number in the dielectric medium. The effective radius R_{de} of the disc is given as [11]

$$R_{de} = R_d \left\{ 1 + \frac{2(h_1+h_2+h_3)}{\pi R_d \varepsilon_{ed}} \left(\log \frac{\pi R_d}{2(h_1+h_2+h_3)} + 1.7726 \right) \right\}^{1/2} \tag{8}$$

The equivalent circuit of the first and second resonators, based on modal expansion cavity model [12], is shown in Figs. 2(a) and (b) from which their impedances can be derived as

$$Z_{ANNULAR} = \frac{j\omega L_1 R_1}{R_1 - \omega^2 L_1 C_1 R_1 + j\omega L_1} \tag{9}$$

and

$$Z_{DISC} = \frac{j\omega L_2 R_2}{R_2 - \omega^2 L_2 C_2 R_2 + j\omega L_2} \tag{10}$$

The resistance R_1, inductance L_1 and capacitance C_1 of the annular ring are calculated as [8]. R_2, L_2 and C_2 are the resistance, inductance and capacitance of the disc respectively and these are calculated as [12].

These two resonators couple together through electromagnetic coupling to provide broadband operation to the proposed antenna.

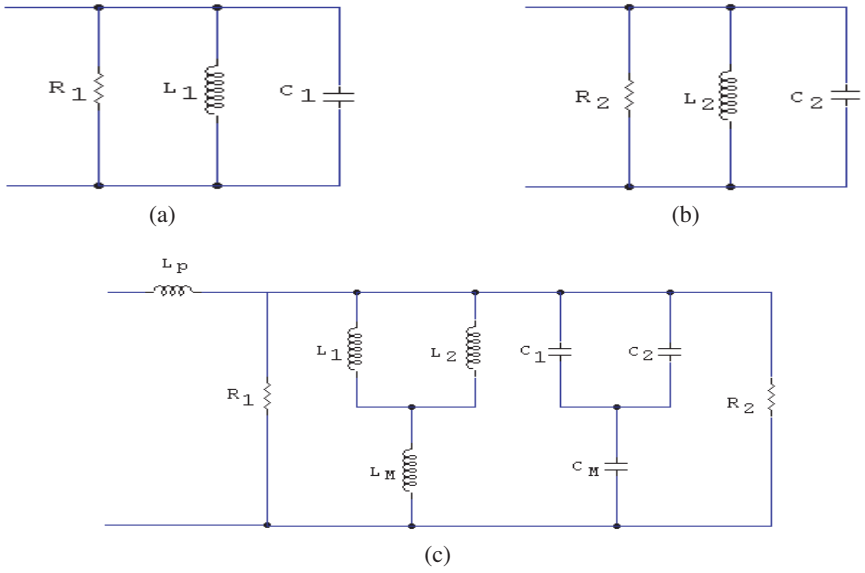

Figure 2. (a) Equivalent circuit of first resonator, (b) Equivalent circuit of second resonator, (c) Equivalent circuit of the proposed antenna.

If c_p be the coupling factor, the mutual inductance L_M and mutual capacitance C_M are given as

$$L_M = \frac{c_p^2 (L_1 + L_2) + \sqrt{c_p^4 (L_1 + L_2)^2 + 4c_p^2 \left(1 - c_p^2\right) L_1 L_2}}{2\left(1 - c_p^2\right)} \quad (11)$$

$$C_M = \frac{-(C_1 + C_2) + \sqrt{(C_1 + C_2)^2 - C_1 C_2 \left(1 - \frac{1}{c_p^2}\right)}}{2} \quad (12)$$

The equivalent circuit of the proposed antenna is shown in Fig. 2(c). From this figure, the impedance of the proposed antenna can be derived as

$$Z_{in} = j\omega L_P + \frac{\omega^2 R_T L_T^2 + j\omega R_T^2 L_T \left(1 - \omega^2 L_T C_T\right)}{\omega^2 \left(\omega^2 R_T^2 L_T^2 C_T^2 - 2R_T^2 L_T C_T + L_T^2\right) + R_T^2} \quad (13)$$

where $R_T = \frac{R_1 R_2}{R_1 + R_2}$, $L_T = \frac{L_1 L_2}{L_1 + L_2}$, $C_T = \frac{(C_1 + C_2) C_M}{C_1 + C_2 + C_M}$ and L_P is the inductance due to the co-axial probe of 50 ohm.

The return loss (RL) of the antenna is given as

$$RL = 20\log_{10}|\Gamma|, \quad \Gamma = (Z_{in} - Z_0)/(Z_{in} + Z_0) \tag{14}$$

where Z_0 is the characteristic impedance of the feeding line (50 ohm).

As there exists electromagnetic coupling between the fed patch and the parasitic patch, the radiation from the proposed antenna is contributed by the coupling between them. Therefore, for the far-field radiation of the proposed antenna, following assumptions can be made.

1. The slot voltage induced in the parasitic patch is c_p times the slot voltage of the fed patch.
2. The radiations from the two patches can be considered to be in the same phase because the gap between the fed patch and the parasitic patch are very small as compared to the far-field point.

Hence the radiated far-field of the proposed antenna can be given as

$$E_\theta = E_\theta^{ANNULAR} + E_\theta^{DISC} \tag{15}$$

$$E_\phi = E_\phi^{ANNULAR} + E_\phi^{DISC} \tag{16}$$

where the radiation field for fed annular patch are given as [10]

$$E_\theta^{ANNULAR} = \frac{j^n 2hk_0E_0}{\pi\, k_{nm}} \frac{e^{-jk_or}}{r} \left[J_n'(k_0a\sin\theta) - J_n'(k_0b\sin\theta)\frac{J_n'(k_{nm}a)}{J_n'(k_{nm}b)} \right] \cos n\phi \tag{17}$$

$$E_\phi^{ANNULAR} = \frac{-j^n 2nhk_0E_0}{\pi\, k_{nm}} \frac{e^{-jk_or}}{r} \left[\frac{J_n(k_0a\sin\theta)}{k_0a\sin\theta} - \frac{J_n(k_0b\sin\theta)}{k_0b\sin\theta}\frac{J_n'(k_{nm}a)}{J_n'(k_{nm}b)} \right] \cos\theta \cdot \sin n\phi \tag{18}$$

and the radiation field for the parasitic disc are given as [11]

$$E_\theta^{DISC} = \frac{j^n k_0R_dc_pV_0}{2} \frac{e^{-jk_0r}}{r} [J_{n+1}(k_0R_d\sin\theta) - J_{n-1}(k_0R_d\sin\theta)] \cos n\phi \tag{19}$$

$$E_\phi^{DISC} = \frac{j^n k_0R_dc_pV_0}{2} \frac{e^{-jk_0r}}{r} [J_{n+1}(k_0R_d\sin\theta) + J_{n-1}(k_0R_d\sin\theta)] \cos\theta \cdot \sin n\phi \tag{20}$$

where $V_0 = hE_0J_n(kR_d)$ is the radiating edge voltage, and r is the distance of an arbitrary far-field point. k_0 and k_{nm} are the propagation constant in free space and dielectric medium respectively in TM_{nm} mode.

3. CALCULATIONS AND DISCUSSION OF RESULTS

The calculations of return loss for different parameters were accomplished using Equation (14); the resulting data are shown in Figs. 3–6. Fig. 3 shows the variation of return loss with frequency at

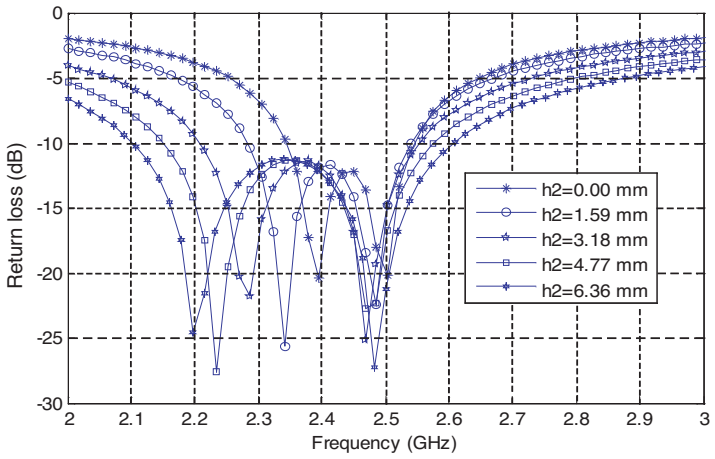

Figure 3. Variation of return loss with frequency at different air-gap spacing (h_2).

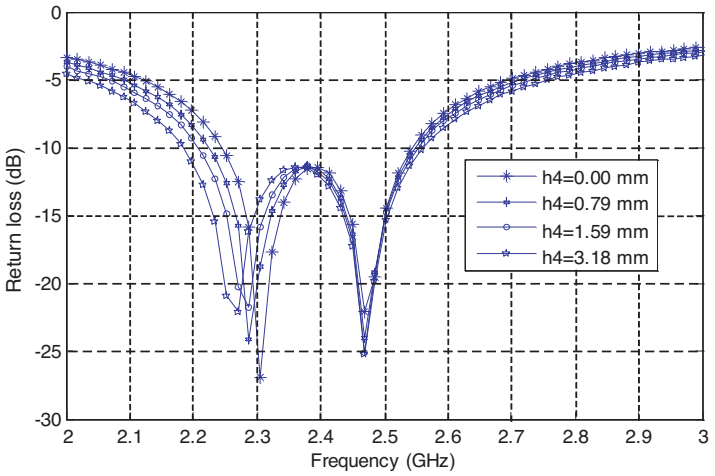

Figure 4. Variation of return loss with frequency at different superstrate thickness (h_4).

different air-gap spacing (h_2). It is observed that in the absence of air-gap, the antenna shows an impedance bandwidth of 8.75% with two resonance frequencies at 2.396 GHz and 2.504 GHz respectively. The inserting of air-gap between the fed and the parasitic patches improves, significantly, the performance of the antenna. It is found that the frequency band of operation of the proposed antenna increases from 257.8 MHz (bandwidth 10.68%) to 501.2 MHz (bandwidth 21.42%) with increasing air-gap spacing from $h_2 = 1.59$ mm to $h_2 = 6.36$ mm. A significant decrease in the lower resonance frequency is observed with increasing h_2 whereas higher resonance frequency is almost invariant. The effect of substrate thickness (h_4) on the antenna performance is shown in Fig. 4. It is found that the incorporation of superstrate on the parasitic patch improves the bandwidth of the proposed antenna on the one hand but it causes mismatching at two resonance frequencies by decreasing resonance resistance, on the other hand. The bandwidth of the proposed antenna increases up to 13.96% with increasing superstrate thickness to $h_4 = 3.18$ mm whereas the antenna has 10.89% bandwidth without superstrate. The superstrate also affects the two resonance frequencies in which the lower resonance frequency decreases considerably from 2.252 GHz to 2.198 GHz and the higher resonance frequency shows a little shift with h_4.

Figure 5 shows the performance of the proposed antenna at

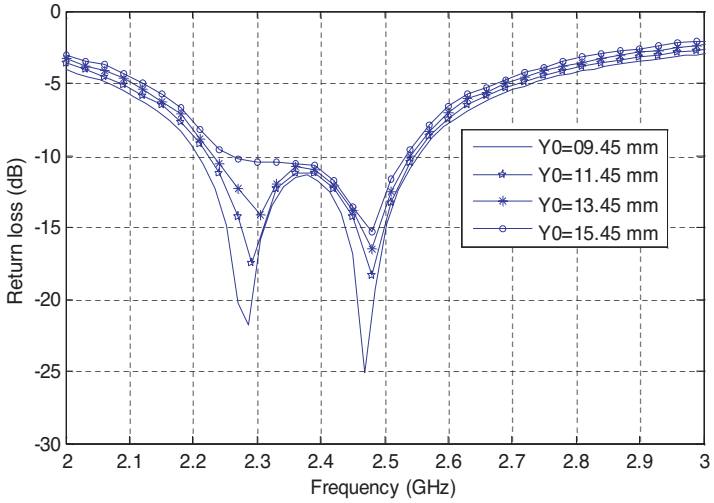

Figure 5. Variation of return loss with frequency at different feeding point location (Y_0).

different feeding point locations (Y_0). It depicts that the proposed antenna is very sensitive to the feeding point location working on TM_{11} mode whereas a single annular ring microstrip antenna is independent of feeding point location as reported by Lee and Dahele [1, 13]. It is observed that displacement of feed point from inner periphery of the ring towards outer periphery causes considerable mismatching at lower resonance frequency and moderate mismatching at higher resonance frequency. For the comparative study of theoretical, simulated and

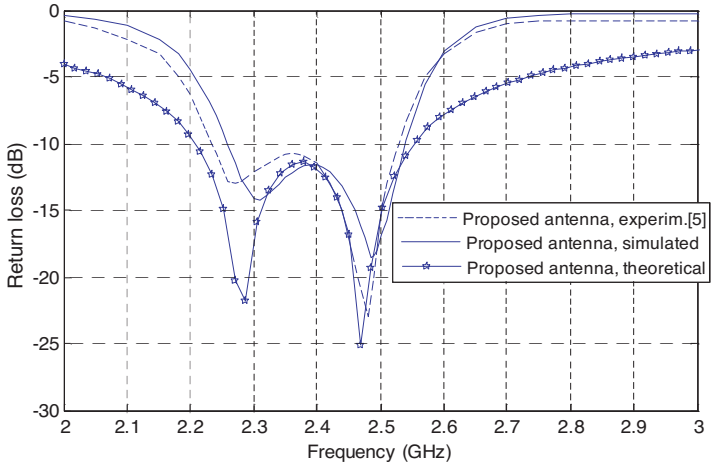

Figure 6. Optimized return loss curve of the proposed antenna.

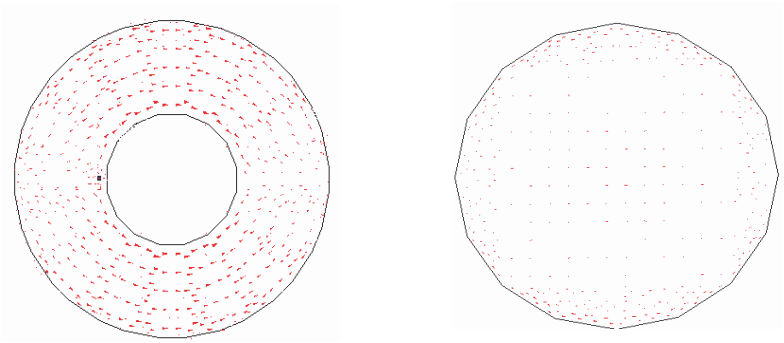

Figure 7. Current distributions at frequency 2.30 GHz (a) fed patch (b) parasitic patch.

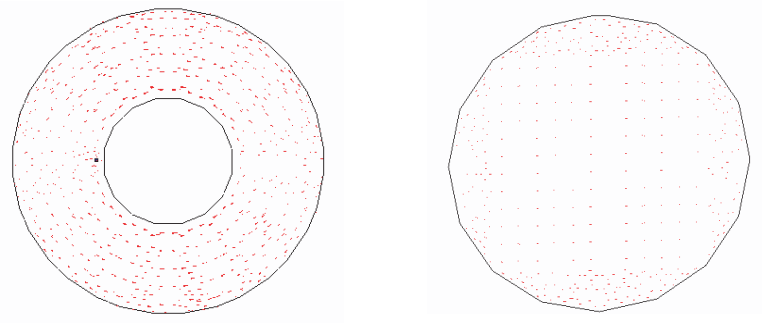

(a) (b)

Figure 8. Current distributions at frequency 2.49 GHz (a) fed patch (b) parasitic patch.

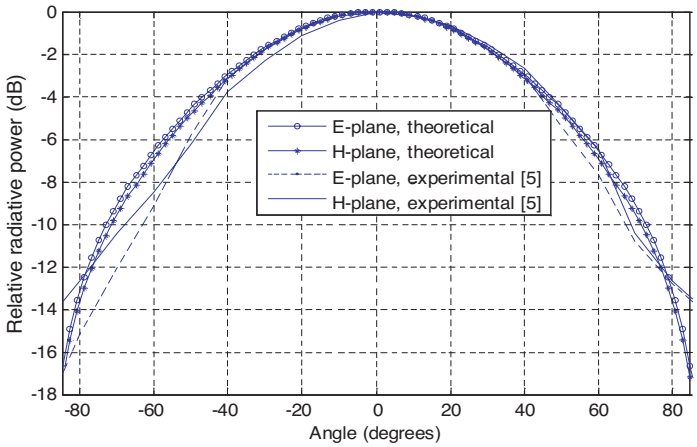

Figure 9. Radiation pattern of the proposed antenna at frequency 2.23 GHz.

experimental [5] results, the optimized return loss curves for the proposed antenna are shown in Fig. 6 as a function of frequency. It is pointed out that the theoretical results are in excellent agreement with the simulated and experimental [5] results. These justify the veracity of the proposed method. The simulated current distributions at different frequencies are presented in Figs. 7 and 8. It is observed that the effect of the parasitic patch is very significant at the two frequencies. The magnitude of currents in the parasitic patch is contributed by the electromagnetic coupling through air-gap between the two patches.

The calculations for E- and H-plane radiation patterns of the

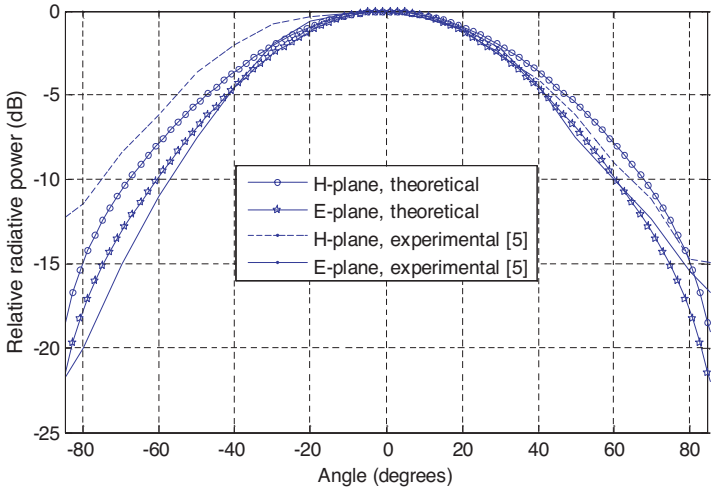

Figure 10. Radiation pattern of the proposed antenna at frequency 2.53 GHz.

proposed antenna were carried out using Equations (15)–(20); the data so obtained are shown in Figs. 9 and 10. These figures depict that the theoretical radiation patterns at 2.230 GHz and 2.530 GHz are very close to the experimental radiation patterns at that frequencies. It is found that the 3-dB beam widths of E- and H-plane radiation patterns at frequency 2.230 GHz are 81.4° and 80.2° respectively. Moreover, 66.2° and 74.4° beam widths of E- and H-plane patterns are obtained at 2.530 GHz, respectively.

4. CONCLUSIONS

It is, therefore, concluded that the air-gap spacing, superstrate thickness and feeding point location have crucial effects on the performance of the proposed antenna. The proposed antenna has frequency band of operation of 332 MHz (bandwidth 13.96%) that can be applied in the industrial, scientific and medical (ISM) areas.

REFERENCES

1. Dahele, J. S. and K. F. Lee, "Characteristics of annular ring microstrip antenna," *Electronics Letters*, Vol. 18, No. 24, 1051–1052, Nov. 1982.

2. Liu, H. and X. F. Hu, "Input impedance analysis of microstrip annular ring antenna with thick substrate," *Progress In Electromagnetics Research*, PIER 12, 177–204, 1996.
3. Lee, K. F. and J. S. Dahele, "Two layered annular ring microstrip antenna," *International Journal of Electronics*, Vol. 61, No. 2, 207–217, 1986.
4. Fan, Z. and K. F. Lee, "Input impedance annular ring microstrip antennas with dielectric cover," *IEEE Trans. Antenna Propagat.*, Vol. 40, No. 8, 992–995, Aug. 1992.
5. Al-Charchafchi, S. H., W. K. W. Ali, and S. Sinkeree, "A stacked annular ring microstrip patch antenna," *IEEE Antenna Propag. Society Int. Symp.*, Vol. 2, 948–951, Jul. 1997.
6. Misra, S. and S. K. Chowdhury, "Concentric microstrip ring antenna: Theory and experiment," *Journal of Electromagnetic Waves and Applications*, Vol. 10, No. 3, 439–450, 1996.
7. Garcia, Q. G., "Broadband attacked annular ring," *IEE Antenna and Propogation Conference*, No. 407, 508–512, Apr. 1995.
8. Ansari, J. A., R. B. Ram, S. K. Dubey, and P. Singh, "A frequency agile stacked annular ring microstrip antenna using a Gunn diode," *Smart Materials and Structures*, Vol. 16, 2040–2045, 2007.
9. Liu, Z. F., P. S. Kooi, L. W. Li, M. S. Leong, and T. S. Yeo, "A method for designing broad-band microstrip antennas in multilayered planar structures," *IEEE Trans. Antenna Propagat.*, Vol. 47, No. 9, 1416–1420, Sept. 1999.
10. Garg, R., P. Bhartia, I. Bahl, and A. Ittipiboon, *Microstrip Antenna Design Handbook*, Artech House, Norwood, MA, 2001.
11. Derneryd, A. G., "Analysis of the microstrip disc antenna element," *IEEE Trans. Antenna Propagat.*, Vol. 27, No. 5, 660–664, 1979.
12. Bahl, I. J. and P. Bhartia, *Microstrip Antenna*, Artech House, Bostan, MA, USA, 1980.
13. Lee, K. F. and J. S. Dahele, "Theory and experiment on the annular ring microstrip antenna," *Ann. Telecomm.*, Vol. 40, No. 9, 508–515, 1985.